NULL SPACE IN THE HODGKIN-HUXLEY EQUATIONS

A CRITICAL TEST

E. N. BEST, *The Departments of Aeronautics/Astronautics and Biological Sciences, Purdue University, Lafayette, Indiana 47907 U.S.A.*

ABSTRACT Voltage perturbation methods based upon topological concepts are used to elicit responses from the Hodgkin-Huxley (HH) nonlinear differential equations. These responses present a critical check upon the validity of the HH model for electrical activity across squid axon membrane. It is shown that when a constant current is applied such that a stable equilibrium and rhythmic firing are present, the following predictions are inherent in the HH system of equations: (*a*) Small instantaneous voltage perturbations to the axon given at points along its firing spike result in phase resetting curves (when new phase versus old phase is plotted) with an average slope of 1. (*b*) A larger voltage perturbation (from certain points along the firing spike) results in the permanent cessation of periodic firing, with membrane voltage rapidly approaching the equilibrium value. (*c*) A still larger perturbation yields phase resetting curves with an average slope equal to 0. These predictions, coupled with Tasaki's experimental demonstration that squid axons in excellent condition do give repetitive firing under constant current, provide a critical test of the validity of the HH model.

INTRODUCTION

In 1952, Hodgkin and Huxley published the results of many years of work on the dynamic behavior and physiology of nerves (1, 2). Their work describes experimental procedures and results from the study of giant nerve axon taken from squid. Their paper culminates with a quantitative description of the axon's dynamic behavior in terms of the membrane current density, membrane potential difference, sodium activation and inactivation, and potassium inactivation. Hodgkin and Huxley's quantitative description takes the form of four coupled first-order nonlinear ordinary differential equations with time as the independent variable. No explicit general analytical solution to these equations is known.

This paper applies the theory and search methodology of Winfree to the rhythmic behavior of the Hodgkin and Huxley equations under current constraints that induce periodic firing (3). Since 1968, Winfree, via his interest in biological clock works and cycling phenomena (rhythms), has developed a theory involving a methodology for studying phase resetting patterns of rhythmic systems (4–7). The methodology involves application of patterned perturbations to a periodic cycling system. If the system gives certain specific phase angle changes in response to patterned perturbations, then there are strong topological arguments for the existence of a critical stimulus level and timing for a perturbation such that new phase of the system after the perturbation is indeterminate. In rough terms, the system's typical behavior is disrupted and does not return or at least does not return in a normal manner: "It

---

Dr. Best is currently with the Institute for Science and Humanism, 501 West Mariposa, El Segundo, Calif. 90245.

doesn't know what to do." Biological experiments with the cyclic behavior of fruit flies (7) and yeast (6) have shown that rhythmic behavior under critical perturbations has stopped completely or returned to its normal periodic cycling only after some unpredictable interval. Although the arguments were originally developed from biological experiments, the arguments are topological in nature and can be applied to any periodic cycling system that gives certain key phase angle changes in response to systematic perturbation.

There are two key conceptual approaches to the application of Winfree's idea. First there are the theoretical concepts revolving around limit cycles and the presence of null space. Second, there are experimental procedures that can be applied to a cycling system to determine (via phase resetting curves) whether or not a unique type of response is available from that system. The main idea in the experimental approach is to develop phase resetting curves (new phase versus old phase) for the cycling system and to watch for a transition from one type of characteristic response to another in the resetting curves. The cycling system has some innate period. The phase resetting curves are generated by perturbing the system at uniform intervals during its cycle and recording (for each perturbation) what new phase the system acquires at unit time intervals of its period after the perturbation. A type 1 response is where the average slope of the resetting curve is equal to 1 while the average slope of a type 0 response curve is equal to 0. The key characteristic we look for in the phase resetting curves is a change from a type 1 to a type 0 response. Examples of type 1 and type 0 phase resetting curves are given in Fig. 1. Perkel, in studying the effects of inhibitory or excitatory potential impulses on the activity of crawfish nerves, recorded a type 0 phase resetting curve of the kind illustrated in Fig. 1 (8).

In a type 1 curve, the response is such that during one cycle of old phase (i.e., change of value from 0 to 1), new phase also covers one complete cycle running from 0 to 1; the average slope is equal to 1. During one complete cycle of old phase in the type 0 response, new phase does not necessarily cover one complete cycle and the average slope is equal to 0. In the example shown for a type 0 response in Fig. 1, new phase covers only a subset of the possible range of 0 to 1. With the experimental approach, the system is perturbed and phase resetting curves are obtained. The key is to look for a transition from a type 1 to a type 0 response. Initially, with a perturbation of very small magnitude, we know the response from the system will be a type 1. (In the limit, as perturbation magnitude goes to 0, there is no change. New phase equals old phase/slope equals 1.) We slowly increase the magnitude of the perturbation

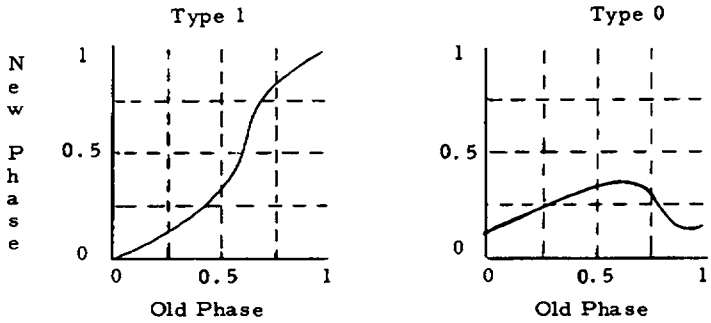

FIGURE 1 Examples of type 1 and type 0 phase resetting curves.

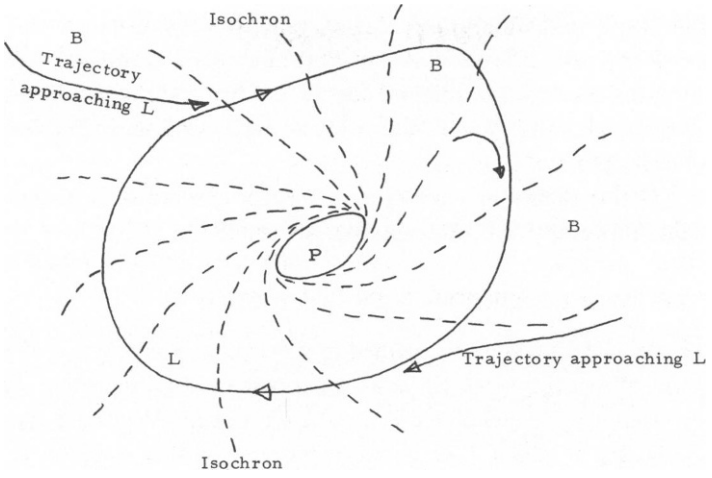

FIGURE 2 Illustration of a limit cycle, L, in an attractor basin, B, with isochrons foliating B and a phaseless set P.

and watch the shape of the phase resetting curves. If there is a transition from the type 1 to a type 0, then we know we have crossed over a critical area in the dynamic response of the preparation; now there are strong topological arguments (9) to indicate that a very dramatic response should be available. It is this dramatic response which I am looking for in the response of real squid axon.

The second approach is through the application of Winfree's limit cycle theory itself. A statement of Winfree's limit cycle theory might be given as follows: consider a dynamic system defined in a continuous space, C, of dimension N. The system's structure is one of a periodic limit cycle, L, which is an attractor surrounded in space by an attractor basin, B. The system's dynamic behavior may be viewed as a smooth progression or flow in time around its limit cycle. Points off the limit cycle in the attractor basin asymptotically approach the limit cycle in time. L is a subset of B, which is a subset of the whole continuous space C.

The limit cycle has some innate period. This period is normalized so that any phase on the cycle can be represented by a number between 0 and 1 (0 and 100% completion of the period from any arbitrary marker point). Then latent phase for any point (state) in the attractor basin, B, can be defined by observing the point at (and only at) unit intervals of time where the intervals correspond to the period of the cycle. The latent phase is then defined as that phase of the limit cycle at which the point is seen as approaching via these glimpses at unit time intervals. Then an isochron may be defined as a line (an N-1 dimensional manifold in a general N-dimensional space) of constant phase in B space composed of the set of those points that approach a given phase point on the limit cycle in unit intervals of time.

With the above definitions and conditions, the specifics of Winfree's theory may be stated as follows (with a two-dimensional example in Fig. 2):

(*a*) The isochrons whose phase value correspond to points in the limit cycle, L, foliate the attractor basin, B.

(*b*) Defining $P = C - B$, where P is the null space ($P < C$), P is not empty and has dimension $\geq N$-2.

(*c*) If K is any "cap" on the limit cycle, L (i.e., any two-dimensional surface bounded only by L), then every K contains at least a point of P. In this sense, part of P "threads" L.

(*d*) If d denotes the boundary of the null space, P, d has co-dimension to C of 1 or 2. Like P, it consists of trajectories that do not return to the limit cycle, L. Every isochron enters the neighborhood of every point of d.[1]

The first proof of this theory has been recently accomplished by J. Guckenheimer of the Math Department, University of California, Santa Cruz (9).

PURPOSE AND DESCRIPTION OF RESEARCH

The Hodgkin-Huxley (HH) equations defined in a 4-D continuous space of V, M, N, and H and under the current restriction which induces periodic cycling, represent a system with the characteristics of a limit cycle embedded in an attractor basin. Winfree's theory predicting a null space is applicable to them. The primary purpose of this research is to identify the subspace (the null space) of the HH equations where the characteristic of flow around the limit cycle or flow toward the limit cycle is absent. In particular, phases of the limit cycle ("portals") will be specified from which voltage perturbations will carry the system away from dynamic cycling and into the null space. This provides the biologist with an immediate opportunity to apply similar voltage perturbation at the same phase of the limit cycle for real squid axon to see if real axon responds in a similar matter.

Although not a primary purpose of the research, I identify this perturbation method as a crucial check on proposed models for repetitively firing nerves. This method can be used to check phase resetting curves and possible null space access portals of any well-behaved system of equations against real nerve phase resetting behavior. The result is solely dependent upon the topology of the model's mathematical structure. It is unlikely that a model will be built with a phase resetting structure in mind. Thus the method presents a critical check on the model's predictability.

One crucial aspect regarding the importance of the research presented here is contained in the repetitive firing of real squid axon. The HH equations clearly give repetitive firing, as illustrated by Fitzhugh (3). For any comparison of phase resetting curves and null space access from the HH equations against the behavior from a real axon, the real axon must be capable of producing more than several repetitive voltage peaks. Examination of the literature and communication with researchers in the field raise some uncertainty as to the number of the repetitive spikes one can expect from real squid axon under constant current. As shown by the work of Guttman and Barnhill (10), it is clear that axon bathed with reduced calcium content solution instead of sea water gives long strings of repetitive firing under constant current or without current if the calcium content is reduced enough. Also, Huxley has produced modifications to the original HH equations to represent squid axon activity when the calcium content of the external solution is reduced (11). However, for squid in normal sea water solution, the literature is uncertain on this question, as indicated by Fitzhugh (3). To clarify this question, I contacted I. Tasaki of the National Institutes of Health in May of 1976. It was his opinion that if the squid axon was in excellent condition, it would give more

[1] As a point of exactness: $d \leq P$. If dim P = N, then $d < P$. But if dim $P < N$, then P is "infinitely" thin and P and its boundary d are identical, $d = P$.

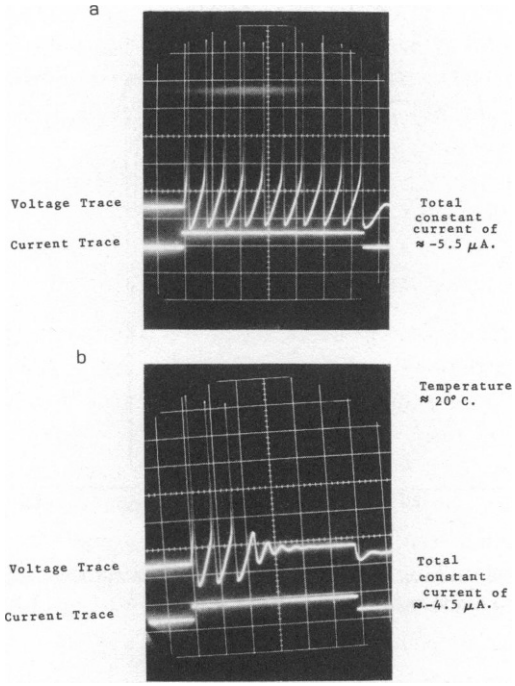

FIGURE 3 Repetitive firing under constant current by squid axon bathed in seawater. Photographs from I. Tasaki, May 1976.

than several repetitive firing cycles under constant current. At that time he ran a constant current experiment on squid axon. The results are shown in Fig. 3.

The oscilloscope photographs shown in Fig. 3 clearly show a transition effect for repetitive firing as a function of current level applied. Negative variation in current and voltage is displayed upward. In Fig. 3 *a* there are 10 voltage firing peaks during the time of application of the constant current. In 3 *b*, with a slight reduction in the current magnitude, there are three diminishing firing peaks followed by subthreshold oscillation approaching a steady-state position. This behavior of the squid axon is qualitatively duplicated by the HH equations. Fig. 4 shows the same sort of transition effect in the number of repetitively firing peaks for the HH equations as the current magnitude increases.

I. Tasaki provided the following data for the photographs in Fig. 3. The axon used was approximately 600 μm in diameter. The length along the axon exposed to the constant current was 10 mm. The temperature was about 20°C. The large division marks on the scope are 10 ms per division, 18 mV per division, and 10 μA per division. The current is total current applied to the axon, not current per unit area.

The current densities that produced repetitive firing in the real axon (-24 $\mu A/cm^2$ and -29 $\mu A/cm^2$) are several times the value (approximately -8.7 $\mu A/cm^2$) that produced the transition to steady-state repetitive firing for the HH equations at 20°C. As indicated by the work of Guttman, there is considerable variation in the magnitude of various properties, such as resting voltage and current level, required to induce firing among individual axons (10). This might be used to explain some of the discrepancy between the current values for Tasaki's

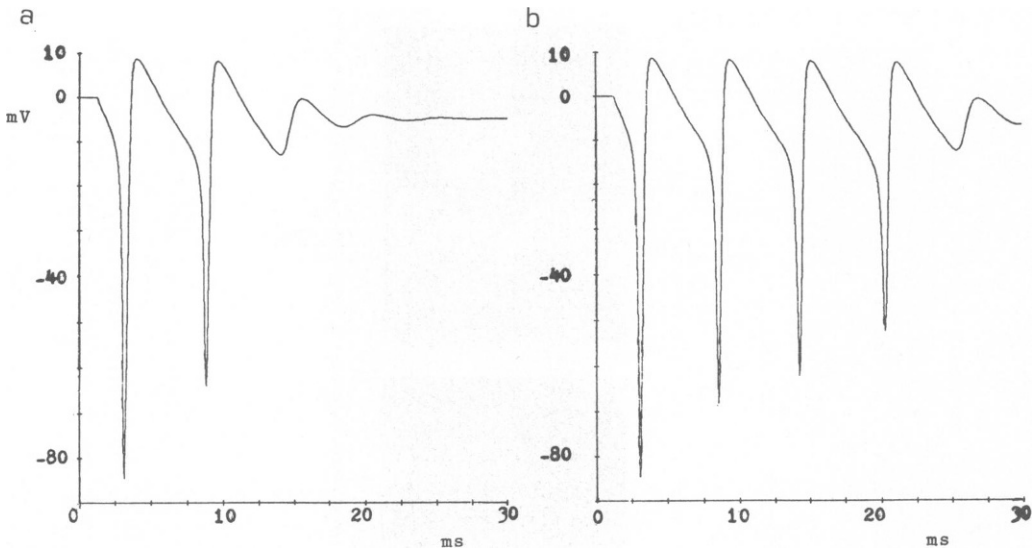

FIGURE 4 HH equations: response of resting axon to a constant current I applied at $T = 1$ ms with a temperature of 20°C. Constant cycling for $I \leq -8.8$ $\mu A/cm^2$. (*a*) $I = -8.5$ $\mu A/cm^2$. (*b*) $I = -8.7$ $\mu A/cm^2$.

repetitive firing axon and the current values given by the HH equations to induce firing. But more importantly, according to Tasaki, the squid which Hodgkin and Huxley used in their experiments were in very poor condition and the current flows now recorded in similar experiments with squid are several times greater.

The HH equations qualitatively duplicate the cycling form and pattern of the voltage response of the healthy squid axon once its own individual critical level of constant current is reached. Winfree's perturbation method is used to give phase resetting curves and to find phase ranges along the HH limit cycle from which the null space is accessible using voltage perturbations. Using this data, biologists should be able to apply voltage stimuli at specified positions on the real axon voltage waveform for a check. With this check it should be easy to confirm if there are certain critical stimuli that stop axon cycling and whether or not squid axons have the phase resetting patterns predicted by the HH equations.

BASIC PROPERTIES OF THE HODGKIN-HUXLEY EQUATIONS

The now familiar equations of Hodgkin and Huxley for electrical activity in a space-clamped squid axon with constant current are presented below. The analysis presented in this paper was performed using exactly these equations with the current parameter "I" set to such values that a repetitive firing sequence was elicited from the equations.

$$I = C_M(dV/dt) + g_K N^4(V - V_K) + g_{NA} M^3 H(V - V_{NA}) + g_L(V - V_L).$$

$$(dM/dt) = A_m(1 - M) - B_m M.$$

$$(dN/dt) = A_n(1 - N) - B_n N.$$

$$(dH/dt) = A_h(1 - H) - B_h H.$$

$$A_m = \frac{0.1(V+25)}{\left[\exp\left(\frac{V+25}{10}\right)-1\right]}. \qquad B_n = 0.125\exp(V/80).$$

$$B_m = 4\exp(V/18). \qquad A_h = 0.07\exp(V/20).$$

$$A_n = \frac{0.1(V+10)}{\left[\exp\left(\frac{V+10}{10}\right)-1\right]}. \qquad B_h = \frac{1}{\left[\exp\left(\frac{V+30}{10}\right)+1\right]}.$$

$C_M = 1.0$ Membrane capacitance in $\mu F/cm^2$.

$V_{NA} = -115$ mV. $g_{NA} = 120$ mmho.

$V_K = +12$ mV. $g_k = 36$ mmho.

$V_L = -10.59892097$ mV. $g_L = 0.3$ mmho.

V_L's extended value was calculated so total ionic current computed is zero at the resting potential ($V = 0$). Potential V is given in millivolts, current density I in microamperes per square centimeter, conductances g in milli-mho's per square centimeter, capacity C_M in microfarads per square centimeter, and time in milliseconds. The expressions for the A's and B's are appropriate to a temperature of 6.3°C. For other temperatures they must be scaled by a factor of $_3[(T - 6.3)/10)]$.

Since the purpose of this research is to provide a check on the HH equations that the biologist can readily make, the most desirable position is to provide him with a case where the equations show a null space. The HH equations have a limit cycle only for a certain range of current value. As the current value changes, the stability of the equilibrium position changes. This is of critical importance. Winfree's theory guarantees that there is a null space when a limit cycle is present, but only guarantees a null space dimension of $N - 2$, which is equal to two for the four dimension HH space. The equilibrium point (which must be within the null space, since derivatives are 0 there and there is no movement toward the limit cycle) can be evaluated analytically and perhaps provide hints to the character of the rest of the null space. The strongest case to give the biologist is the one where the null space is 4-D stable. Solving the HH equations (with derivatives set equal to 0) yields the result that, for each value of current I, there is one and only one set of values for V, M, N, and H for the equilibrium position (12). Thus when a current value is chosen that produces a stable limit cycle in the HH equations, there are only two stable attractor bodies in the state space. These are the limit cycle and the equilibrium point. The null space is defined to be all of the state space, except the attractor manifold for the limit cycle. Thus for the HH equations the null space is equivalent to the attractor manifold (and its boundary) for the equilibrium point.

Information about the equilibrium point and the immediately surrounding null space can be obtained from investigating the equilibrium point's stability properties. These are evaluated by linearizing the original set of equations. Fig. 5 shows how the character of the equilibrium point changes from a stable node to a stable focus and then to an unstable focus as a function of current and temperature.

There appears to be no known way to determine analytically at what current value the limit cycle property appears in the behavior of the complete HH equations. From numerical experiments I have determined that the limit cycle appears in the current range where there is

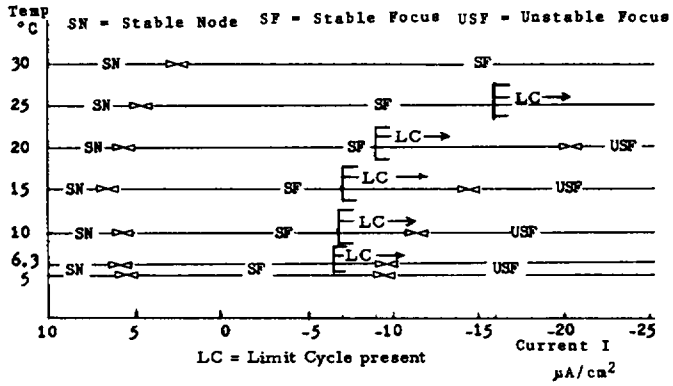

FIGURE 5 Equilibrium characteristics of the linearized HH equations.

a stable focus and continues into the unstable focus region. For example, with a temperature of 20°C, there is a transition from a stable node to a stable focus at a current value of approximately $+6\ \mu A/cm^2$. In the initial region of a stable focus there is no limit cycle present as the current decreases down to a value approximately of -8. At a current value of a -9 there is a limit cycle. The presence of the limit cycle continues into the region of the unstable focus.

In the current region where there is a stable focus it is known that the null space occupies a 4-D space, at least around the area of the equilibrium point. At the current values for an unstable focus the existence of two eigenvalues (with positive real parts) in the solution for the linearized equations and two with negative real parts tells us that the null space around the equilibrium is only 2-D. This corresponds to the minimum dimension of the phaseless set predicted by theory for this set of equations. The HH system, if perturbed into the 4-D null space, could be expected to remain there. If the system is perturbed into a 2-D null space, it could be expected to give some peculiar behavior, but to return eventually to the limit cycle.

For the major part of this research I chose the standard temperature of 6.3°C and a current value of a $-8.75\ \mu A/cm^2$. With this current value there is a limit cycle and the system is still within the region of a stable focus. The null space predicted here by the HH equations is clearly discernible in its behavior from the limit cycle behavior.

NUMERICAL INTEGRATION

The HH equations must be numerically integrated to investigate their behavior. In view of the great amount of numerical analysis and investigation to be done it was important to find and use an accurate and efficient method of integration. Cooley and Dodge, in an investigation of excitation in the HH equations, made use of the modified Euler method of integration (13). Moore and Ramon directly studied the effects of using different integration procedures when evaluating the action potential for the HH equations (14). They evaluated the results by using a Runge-Kutta method, the simple Euler methods, a modified Euler method, a Runge-Kutta method with a partial analytical expression for the variables M, N, and H, and an Adams predictor corrector method. The result of their work was the choice of a simple modification of the Euler method as most efficient and accurate.

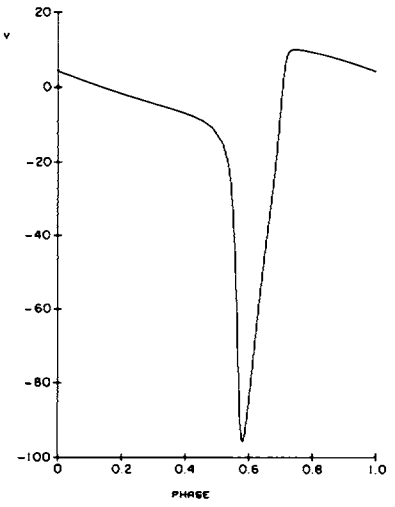

FIGURE 6 Voltage spike (in millivolts) as a function of phase for one complete revolution around the limit cycle. Constant current = $-8.75\ \mu A/cm^2$.

My original intent was to use a Runge-Kutta method. But after reading the article by Moore and Ramon, I decided to investigate the various methods of integration myself. My results directly contradicted those of Moore and Ramon. My choice was the variable step Runge-Kutta integration algorithm with modifications due to England (15, 16). This method was both faster and more accurate than any of the other methods proposed. Not only was this true on the limit cycle portion of the HH state space where the previous work on integration methods was concentrated, but also this was particularly true for operation off the limit cycle, which is the very region where much evaluation is done in search for the null space. It is in this region with very quickly changing system behavior and large derivatives that accuracy was most needed. It was imperative to use a variable step integration scheme that would check on its own accuracy.

Description of Limit Cycle for $I = -8.75$

A standard temperature of 6.3°C is used for all work and graphs. The limit cycle period is 15.413 ms. Phase along the limit cycle is defined as the percent completion of the trip in time around the limit cycle from some arbitrary starting point. The arbitrary starting point on the limit cycle (phase equal 0) is chosen to be $V = 4.82$, $M = 0.030$, $N = 0.450$, and $H = 0.397$. Fig. 6 shows V versus phase, the complete cycle which voltage goes through in one trip around the limit cycle. Since phase is a linear function of time, Fig. 6 could just as well be V versus time with an initial time of 0 and ending time of 15.413 ms.

PHASE RESETTING CURVES AND NULL SPACE ACCESS

In the search for the check on HH equations that biologists can readily make, the critical stimulus approach (seeking the stimulus where there is a transition from a type 1 to type 0 phase resetting response) to the search for the null space is very rewarding. For the limit cycle with a constant current of $-8.75\ A/cm^2$ at a temperature 6.3°C, this approach yields phase

resetting curves and voltage perturbation-phase combinations that show access portals to the null space.

Of the four variables present in the HH equations, voltage is the only one immediately available to the biologist for change. Also, it is the only one possible to change "instantaneously" in the laboratory. So voltage V is the first choice for use in perturbing the equation's cyclic behavior in seeking a critical stimulus. A critical stimulus involving V is a DV (perturbation) of a certain magnitude, sign, and time of application in the cycling, such that the system goes from an initial point $X = (V, M, N, H)$ to a new point $X' = (V + DV, M, N, H)$ with X' being in the null space. For the HH equations, this is accomplished by numerically integrating the equations to the point X, adding DV to the V value to get a new V', and then integrating forward in time from the new point X'. In the laboratory, an equivalent procedure would be to change from a constant current control to a voltage control such that V is changed to $V + DV$ within the neighborhood of a microsecond and then back to a constant current control. R. Fitzhugh has suggested that a more practical way to do the same thing would be merely to inject a brief strong pulse of current ΔI while still under current control.[2] Then $\Delta V \doteq (\Delta I * \Delta T)/C$ for short enough ΔT; since C is independent of V, ΔV is independent for fixed ΔI.

The period for the limit cycle is 15.413 ms (accurate to this many figures). The phase resetting curves presented below were generated by applying the indicated DV to the system at a specified phase ("old phase") of the limit cycle and then integrating forward 15.413 ms. Then the system position of (V, M, N, H) is compared with points on the limit cycle. If the system point was "close enough," such that integrating forward in time would give effectively the same result as integrating forward from a particular point on the limit cycle, then the system point was considered to be "phase captured" and a corresponding "new phase" was calculated and assigned. If the system point was not close enough, then the equations were integrated forward for another time period and another comparison was made. This was repeated until the system was "phase captured" or until it had been determined that the system was approaching the equilibrium position, was trapped in the equilibrium attractor manifold, and hence was in the null space. On the phase resetting curves, such ranges of old phase and DV that yield null trajectories are indicated by a shaded zone. According to theory, at the edges of such a zone all values of new phase should be available. But inside the zone there is no such thing as new phase, since trajectories go to the equilibrium. On the phase resetting graphs, current is indicated by IC and DV, the voltage perturbation by VDELT.

The existence of a null space is indicated by the transition from the type 1 to a type 0 phase resetting curve as the perturbation variable changes in magnitude enough such that all resulting system points from the perturbations are completely beyond the null space. In other words, the portion of the state space that contains the null space has been passed by the perturbations and no other points within the null space can be expected to be encounted by increasing the magnitude of the perturbations still further. Fig. 7 shows the phase resetting curve when a DV of $+2$ mv is applied at uniform intervals along the limit cycle. The phase resetting is a type 1 curve. The average slope across the graph is equal to 1. Figs. 7–10 show a transition from a type 1 response to a type 0 response as null points are encountered and then passed as the DV perturbation is increased beyond $+2$.

---

[2]Fitzhugh, R. Personal communication.

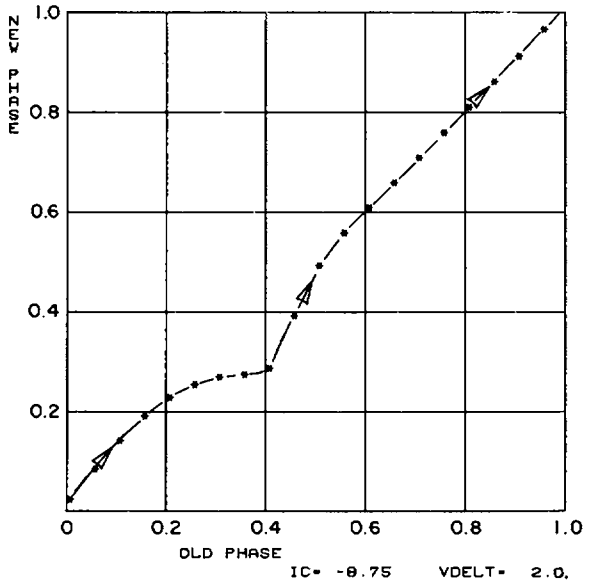

FIGURE 7 Phase resetting curve for $DV = 2$ mV.

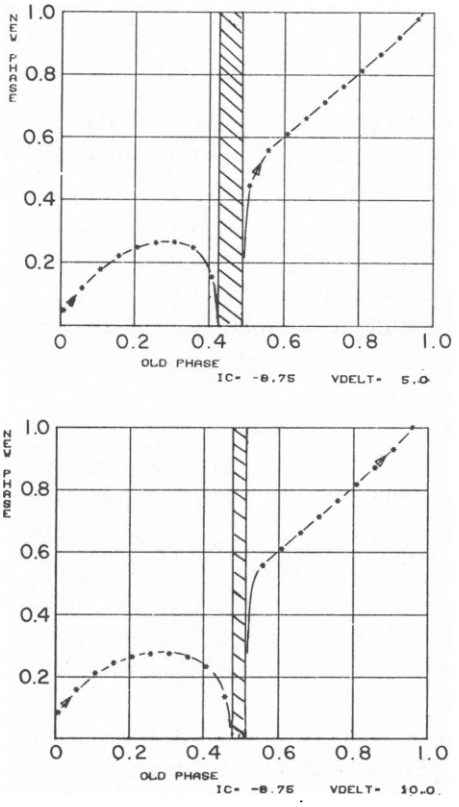

FIGURE 8 Phase resetting curve for $DV = 5, 10$ mV.

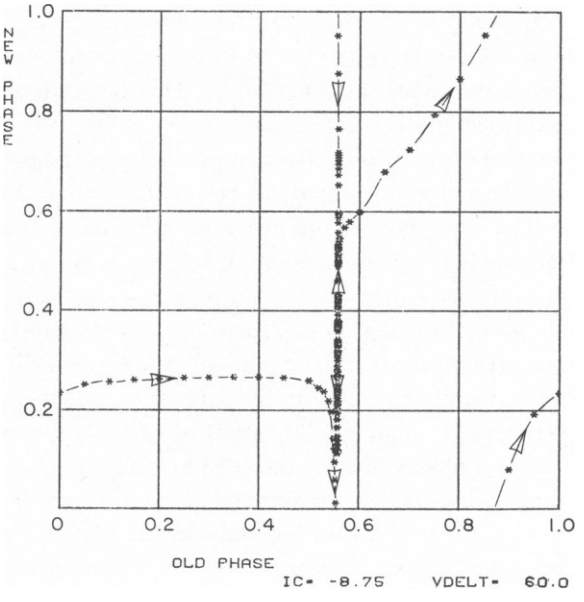

FIGURE 9 Phase resetting curve for $DV = 60$ mV.

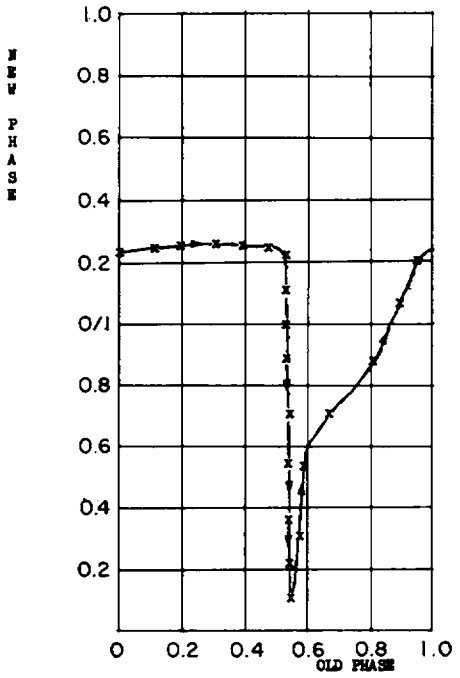

FIGURE 10 Redrawn phase resetting curve for DV = 60 mV.

As the perturbation is increased to 5 and then 10 mv, null points are encountered when the old phase is 0.45 and 0.50, as seen in Fig. 8. Phase resetting results for voltage perturbations of 20 to 50 mv yield plots almost identical to those for VDELT = 60. When DV reaches a magnitude of 20 there are no more null points indicated in the phase resetting curves. However, there appears to be a distinct discontinuity in the phase resetting curve between the old phase values of 0.50 and 0.56. This apparent discontinuity continues as the value of DV is increased and is still present at a DV of 60. This discontinuity was resolved by reducing the interval of old phase between applications of the perturbation. With a large enough resolution, the phase resetting curves are seen to be continuous (Fig. 10).

The continuity of the phase resetting curve seen in Fig. 10 was achieved only after the interval between applications of DV was reduced to 0.30×10^{-11} units of old phase. Since one unit of phase (one limit cycle period) equals 15. + ms, this interval of phase required for showing continuity is equivalent to an exceedingly small increment of time. This might well be one area where the HH equations give biologically unrealistic results. But this will probably remain untested, since in the laboratory the biologist will be unable to create experiments separated by that small amount of time. The most that he will be able to look for is, that between phases of 0.55 and 0.56 on the limit cycle, the HH equations predict an extremely rapid phase shift that covers the whole spectrum from 0 to 1 in new phase.

In Fig. 9 it is not immediately obvious that the phase resetting curve is a type 0 curve, but nevertheless it is. It helps to "see" the 0 average slope of Fig. 9 when it is remembered that on the limit cycle, phase 1 is the same point as phase 0. Thus on the new phase versus old phase graphs, when the curve dips down and goes through the bottom of the graph (new phase

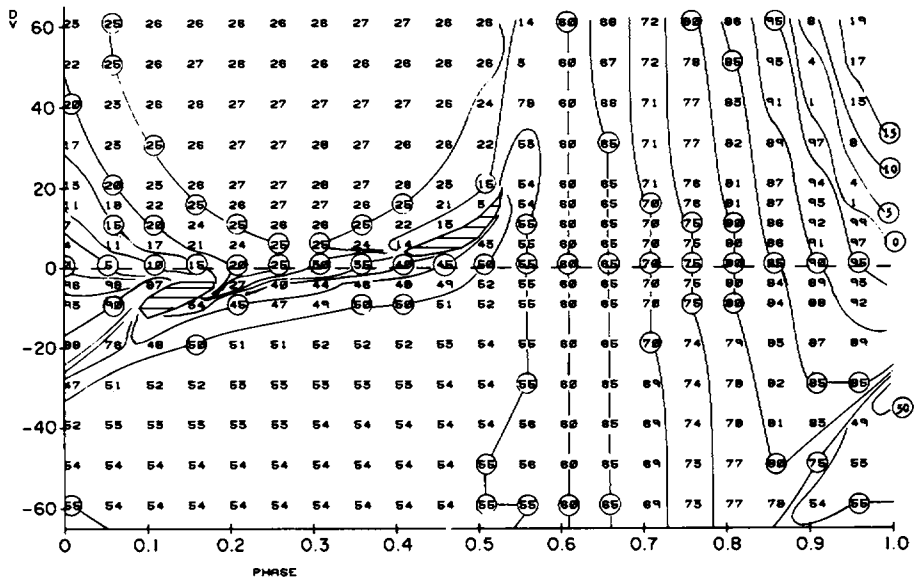

FIGURE 11 Null space access portals (lined areas) and isochrons (in percentage values) as functions of voltage perturbation (*DV*, in millivolts) and phase along the limit cycle. Constant current of -8.75 $\mu A/cm^2$.

equals 0) it continues downward immediately through the top of the graph, since phase 0 is the same as phase 1. Making use of this, Fig. 9 can be redrawn as two "0 to 1" graphs on top of each other. This is done in Fig. 10 with the distance between the descending and ascending portions of the graphs artificially enlarged for clarification. Now with this enlargement it becomes clear that the average slope is indeed 0.

Negative *DV* perturbations were performed in the same manner as the positive perturbations. Initially, null points are encountered for some values of old phase when the perturbations ($DV = -5, -10$) are applied. Then, as the magnitude of the perturbation increases ($DV = -20$ through -60), no more null points are found and there is a shift to a type 0 phase resetting curve. Information from the negative perturbations is incorporated in Figs. 11 and 12. These figures show the total results for both negative and positive *DV* as a mapping of phase resetting results and null space access portals onto a *DV* versus phase plane (or, for Fig. 12, a voltage versus phase plane). Fig. 11 shows the results of all perturbation experiments done with a constant current of a -8.75 A/cm^2. This figure shows the different phase resetting results obtained for applications of various *DV* at various phases along the limit cycle. It also shows two "access portals" into the null space. These two lined areas show combinations of old phase and *DV* such that the result of the application of that *DV* is the system being perturbed into the null space. That is, it does not return to the limit cycle. There is no new phase established.

Theory says that all isochrons (lines of constant latent phase) come arbitrarily close together at the boundary of the null space. This is illustrated in Fig. 11, where the isochrons (as generated by connecting new phase points of the same value) do converge toward the two null space portals. Thus the closer the system is perturbed to the null space, the more potential

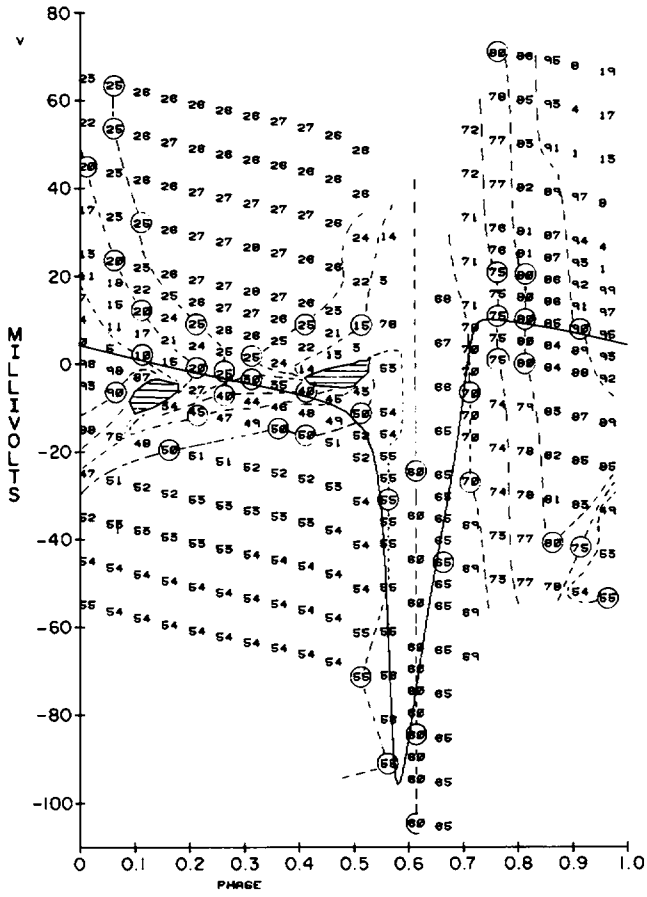

FIGURE 12 Null space access portals (lined areas) and isochrons (in percentage values) superimposed on the limit cycle voltage trace. Constant current of $-8.75\ \mu A/cm^2$.

variation there will be in new phase established when the system goes back to the limit cycle. This results from the fact that it is easier to "hit" a wider range of isochrons (which determine the new phase) when they are packed closely together near the null space.

Fig. 12 shows the same data as Fig. 11. However, here the new phase results and the null access portals are superimposed on the limit cycle voltage trace. Thus Fig. 12 shows where the biologist, in observing the firing spikes of an axon in his own laboratory, could (at the phase of the spike either directly above an indicated null space area or directly below that area) give a perturbation of the appropriate magnitude such that it would "kick" the system into a null space access portal and thus stop the cycling of the axon.

Fig. 13 should be of particular interest, since this is the indicated response the biologist should see on his oscilloscope if the HH equations truly represent what squid axon will do under voltage perturbations. Also the isochrons in Figs. 11 and 12 should be of interest. They provide the resetting character to be expected from squid if the HH equations hold forth. This basic character displayed by the isochrons is a function of the structure of the HH equations and should not drastically change as parameters change.

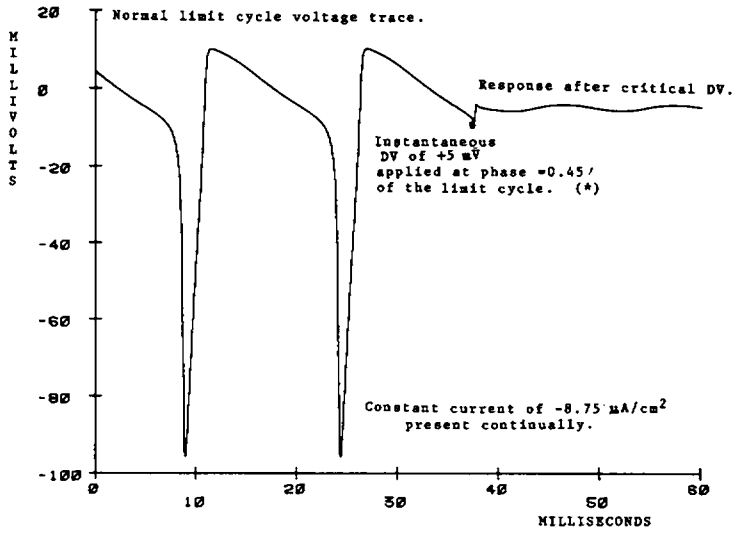

FIGURE 13 Voltage trace from the HH equations before and after a critical perturbation to the normally cycling system.

COMMENTS

This paper's first contribution is an increased understanding of the responses available from the HH model for electrical activity across squid axon membrane and the generation of predictions from the model for real axon behavior. The HH state space is identified as having a limit cycle attractor manifold and an equilibrium attractor manifold that forms the topological basis for the different phase resetting results and null space access portals given in Figs. 11 and 12.

This paper shows that when a constant current is applied such that a stable equilibrium and rhythmic firing are present, the following predictions are inherent in the HH system of equations. Small instantaneous voltage perturbations to the axon given at points along its firing spike result in phase resetting curves with an average slope of 1 (type 1 curves). A larger voltage perturbation (from certain points along the firing spike) results in the permanent cessation of periodic firing, with membrane voltage rapidly approaching the equilibrium value. (Periodic firing can be reinstated, if desired, with a voltage perturbation of magnitude greater than ± 20 mV). A still larger perturbation yields phase resetting curves with an average slope equal to 0. For certain combinations of parameter values the phase resetting curve is very steep (Fig. 9). The above predictions, coupled with Tasaki's experimental demonstration that squid axons in excellent condition do give repetitive firing under constant current, provide a critical test of the validity of the HH model.

In searching for the null space portals indicated in Figs. 11 and 12, the biologist should not be disappointed if the HH predictions turn out to be in error and he finds no null space entrance at the predicted places. By plotting his own phase resetting results in the manner of Figs. 11 and 12, he can determine the location of the null space for his nerve by the convergence of the lines of constant phase. With the number of experiments necessary to generate a figure 12, the biologist might well have to contend with accommodation in a single

squid axon. I would suggest that the stability of the preparation could be checked by periodically seeing if it will duplicate an already generated phase resetting response. But initial work by Guttman et. al. (17, 18) indicates fairly quick success in locating the null space in experimental squid axon.

In the literature there is a continuing misconception that the HH equations demonstrate limit cycle behavior only in the presence of an unstable equilibrium point (Fitzhugh [3], Sabah and Spangler [19]). Cooley and Dodge (13) and Gurel (12) showed that a limit cycle and a stable equilibrium do exist simultaneously. The current value producing a stable equilibrium was used in this work so that the dramatic change in behavior from repetitive firing to a steady-state condition (both under the same constant current) could be illustrated. With the stable equilibrium there is a "stable" equilibrium manifold which, once entered (via the critical perturbations specified in Figs. 8, 11, and 12), allows the system to go nowhere but to the equilibrium. If the limit cycle existed only with an unstable equilibrium, there would not be such distinct behaviors (return to periodic firing versus rapid approach to an equilibrium) predicted by the equations in response to perturbations.

When there is a limit cycle present, theory says that there must also be a null space present and that it can be detected (regardless of its dimension) by a transition from a type 1 to a type 0 phase resetting curve. So with an unstable equilibrium we can expect type 1 and type 0 phase resetting curves similar to those in Fig. 1. However, for the unstable equilibrium case, critical perturbations (those perturbing the system into the null space) would yield trajectories that will return to the limit cycle and thus generate a new phase value. There would be no cross-hatched area (such as Fig. 8 shows) in the phase resetting curves, but I suspect we would find a point along the old phase axis from which a repeated critical perturbation would yield new phase results covering the entire range from 0 to 1 (such as illustrated in Fig. 9 for old phase 0.55).

Preliminary phase resetting results (to be published later) indicate that the size of the null space entrance portals can be increased somewhat by manipulating the current value, temperature, and external calcium level. In particular, the biologist can increase the size of the null space by using a constant current value close to the one which initially produces repetitive firing in the preparation. That is, in reference to Fig. 5, as he reduces current in the negative direction, he would use a value that produces a limit cycle but is as far away as possible from the area of an unstable focus.

The topology of a limit cycle and stable equilibrium embedded in a 2-D space requires the existence of an unstable limit cycle. Cooley and Dodge (13) presented computational results suggesting the existence of an unstable limit cycle for the HH equations when a stable equilibrium and a limit cycle are present. The results generated in my search for the boundary of the null space around the location of the equilibrium strongly suggest the existence of such an unstable limit cycle. For initial points just outside the null space, the resulting trajectories cycle, and only after several revolutions do they rapidly spiral out to the limit cycle. For points just barely within the null space boundary, the resulting trajectories outline the shape of a cyclic path and only slowly at first move away toward the equilibrium.

Although this work has been done with the HH equations, its true importance lies not in the investigation of this particular rhythmic model, but in the presentation of a new area of

inquiry into rhythmic systems with important implications for both experimental and modeling work.

Phase resetting curves or phase-stimulus plots such as Figs. 11 and 12 provide a way of condensing and bringing into view strong dynamical characteristics of a rhythmic system. Any model hoping to truly represent a particular living rhythmic system must be capable of displaying the same resetting characteristics as that biological system. In areas where the basic internal structure and functioning of a particular component of a cycling system is not available to us (such as the squid axon membrane), comparison of resetting qualities between the "black box" experimental object and possible mathematical descriptions offers one avenue for further insight into that "black box." In the area of control mechanisms in biological systems (through limit cycle dynamics), the existence of a null space offers intriguing possibilities.

I would like to thank I. Tasaki for his kindness in responding to my questions about repetitive firing in squid axon by running the constant current experiment and supplying the resulting oscilloscope photographs. Thanks are also particularly due to A. T. Winfree for many hours spent in explaining his theories and for providing constructive criticism and suggestions.

This work was performed as part of the author's doctoral research at Purdue University. Appreciation is also expressed to the Institute for Science and Humanism for providing support in a new creative environment during the writing of this paper.

Received for publication 5 November 1977 and in revised form 23 January 1979.

REFERENCES

1. HODGKIN, A. L., A. F. HUXLEY, and B. KATZ. 1952. Measurement of current voltage relations in the membrane of the giant axon of Loligo. *J. Physiol. (Lond.).* **116**:242–448.
2. HODGKIN, A. L., and A. F. HUXLEY. 1952. A quantitative description of membrane current and application to conduction and excitation in nerve. *J. Physiol. (Lond.).* **117**:500–544.
3. FITZHUGH, R. 1961. Impulses and physiological states in theoretical models of nerve membrane. *Biophys. J.* **1**:445–466.
4. WINFREE, A. T. 1973. Time and timelessness in biological clocks. In Temporal Aspects of Therapeutics. John Urguhart, editor. Plenum Publishing Corporation, New York. 35–57.
5. WINFREE, A. T. 1974. Patterns of phase compromise in biological cycles. *J. Math. Biol.* **1**:73–95.
6. WINFREE, A. T. 1972. Oscillatory glycolysis in yeast: the pattern of phase resetting oxygen. *Arch. Biochem. Biophys.* **149**:388–401.
7. WINFREE, A. T. 1971. Corkscrews and Singularities in Fruitflies: Resetting Behavior of the Circadian Eclosion Rhythm, Biochronometry. National Academy of Sciences, Washington, D.C. 81–109.
8. PERKEL, D. H., J. H. SCHULMAN, T. H. BULLOCK, G. P. MOORE, and J. P. SEGUNDO. 1964. Pacemaker neurons: effects of regularly spaced synaptic input. *Science (Wash. D.C.).* **145**:61–63.
9. GUCKENHEIMER, J. 1975. Isochrons and phaseless sets. *J. Math. Biol.* **1**:259–273.
10. GUTTMAN, R., and R. BARNHILL. 1970. Oscillation and repetitive firing in squid axons. *J. Gen. Physiol.* **55**:104–118.
11. HUXLEY, A. F. 1959. Ion movement during nerve activity. *Ann. N.Y. Acad. Sci.* **81**:221–246.
12. GUREL, O. 1973. Bifurcations in Nerve Membrane Dynamics. *Int. J. Neurosci.* **5**:281–286.
13. COOLEY, J., F. DODGE, and H. COHEN. 1965. Digital computer solutions for excitable membrane models. *J. Cell. Comp. Physiol. 66:99–110.*
14. MOORE, J., and F. RAMON. 1974. On numerical integration of the Hodgkin Huxley equations for a membrane action potential. *J. Theor. Biol.* **45**:249–273.
15. ENGLAND, R. 1969. Error estimates for Runge Kutta type solutions to systems of ordinary differential equations. *Comput. J.* **12**:166–170.

16. SHAMPINE, L. F., and H. A. WATTS. 1970. Efficient Runge Kutta Codes, Sandia Labs, Albuquerque. Report SC-RR-70-615.
17. GUTTMAN, R., and S. LEWIS. 1978. Repetitive firing in squid axon membrane as a model for a neuronal oscillator. *Biol. Bull. (Woods's Hole).* **155**:441.
18. GUTTMAN, R., S. LEWIS, and J. RINZEL. 1979. Control of repetitive firing in squid axon membrane as a model for a neuron oscillator. *J. Physiol. (Lond.).* In press.
19. SABAH, N. H., and R. A. SPANGLER. 1970. Repetitive response of the Hodgkin-Huxley model for the squid giant axon. *J. Theor. Biol.* **29**:155–171.